JOURNAL OF MATERIALS SCIENCE 14 (1979) 312–320

Stress relaxation in hot-drawn low density polyethylene

R. SELDÉN
Department of Polymeric Materials, Chalmers University of Technology, Fack, S-402 20 Gothenburg, Sweden

The tensile stress relaxation behaviour of hot-drawn low density polyethylene, (LDPE), has been investigated at room temperature at various draw ratios. The drawing was performed at 85° C. The main result was an increase in relaxation rate in the draw direction, especially at low draw ratios when compared to the relaxation behaviour of the isotropic material. This is attributed to a lowering of the internal stress. The position of the relaxation curves along the log time axis was also changed as a result of the drawing, corresponding to a shift to shorter times. The activation volume, v, varied with the initial effective stress σ_0^* according to $v\sigma_0^* \approx 10kT$, where $\sigma_0^* = \sigma_0 - \sigma_i$ is the difference between the applied initial stress, σ_0, and the internal stress σ_i. This result supports earlier findings relating to similarities in the stress relaxation behaviour of different solids.

1. Introduction

In earlier works [1, 2] the stress relaxation behaviour of isotropic polyethylene was studied in detail. The present paper aims at reporting stress relaxation behaviour at room temperature for uniaxially hot-drawn low density polyethylene (LDPE). Special interest is devoted to the influence of varying draw ratios on the internal stress level and to the maximum slope of the relaxation curves (stress versus ln time). At low draw ratios, the internal stress value was found to decrease with increasing draw ratio parallel to the orientation direction, while at higher draw ratios this trend was reversed. It is furthermore found that the value of the internal stress is higher perpendicular to the draw direction compared with the values obtained parallel to this direction. These findings agree well with the behaviour in creep [5]. The stress dependence of the activation volume, v, was evaluated from the exponential law region of the relaxation curves and found to vary in inverse proportion to the initial stress according to $v(\sigma_0 - \sigma_i) \approx 10kT$, where σ_0 is the initial stress and σ_i the internal stress, agreeing well with earlier findings [1–4]. The stress dependence of the activation volume was not affected by the draw ratio, nor was an angular dependence found.

Recent communications concerning stress relaxation measurements in oriented polymers can be found in [6–9]. In [9], the relaxation properties of hot-drawn polypropylene were analysed using the stress-aided thermal activation concept. The activation volume was found to be about the same size as the crystalline unit cell. However, the stress dependence of the activation volume was not studied in detail. With regard to the position of the relaxation curves on the log t axis a shift to longer times for oriented specimens is usually observed in the draw direction, compared to the behaviour of the isotropic material [6–9]. In some cases, however, the reverse trend has been found [6]. The present paper shows that the treatment of stress relaxation in oriented polymers may gain considerably from a proper consideration of the rôle played by the internal stress.

2. Theoretical background

2.1. The stress dependence of flow rate

The expressions commonly used for describing the rate of flow in stress relaxation are [1–3, 10]

$$\dot{\sigma} = -Ae^{\sigma^*/F} \quad (1)$$

$$\dot{\sigma} = -B(\sigma^*)^n. \quad (2)$$

© 1979 Chapman and Hall Ltd. Printed in Great Britain.

Equation 1 originates from the theory of stress aided thermal activation. Accordingly, the quantity F is equal to kT/v, with kT denoting the thermal energy and v the volume of activation. $\dot{\sigma} = d\sigma/dt$ is the stress relaxation rate, and $\sigma^* = \sigma - \sigma_i$ the effective stress, i.e. the difference between the applied and the internal stress. F is the slope of the linear σ–ln t region and A a constant. Equation 2, often used for describing the stress dependence of the dislocation (or defect) velocity in crystalline solids [17], finds an increasing application for polymers. B and n are assumed constant during the relaxation process.

As discussed in detail earlier [1–3], Equation 1 applies to the high stress region (initial part) of the relaxation curves, and Equation 2 to the low stress region.

2.2. The activation volume

The activation volume was calculated as a characteristic parameter of the relaxation curves. Its value is obtained from the exponential law, Equation 1, as [11]:

$$v = kT\left(\frac{d \ln \dot{\sigma}}{d\sigma^*}\right)_{T,p} = \frac{kT}{F}. \quad (3)$$

Obviously, the value of v will be constant in the exponential region.

In the power law region, v is obtained as [11]:

$$v = \frac{nkT}{\sigma^*}$$

2.3. Mechanical anisotropy

The mechanical behaviour of a linear elastic (or viscoelastic) solid [12] can be described in terms of a generalized Hookes law:

$$\epsilon_i = S_{ij}\sigma_j \quad (5)$$

where $i, j = 1, 2 \ldots 6$, and S_{ij} are the (time dependent) components of elastic compliances.

The number of independent elastic compliances is five for a transversely isotropic linear elastic solid [13]. For a transversely isotropic linear viscoelastic solid the number of time dependent elastic compliances is also assumed to be five. Defining the 03 axis as the axis of symmetry and the plane of the sheet as the 3, 2 plane, the variation of Young's modulus, E_θ, at an angle θ to the drawing direction in the plane of the sheet is given by

$$\frac{1}{E_\theta} = S_{22}\sin^4\theta + (2S_{13} + S_{44})\sin^2\theta\cos^2\theta + S_{33}\cos^4\theta. \quad (6)$$

The tensile compliances S_{33} and S_{22} are then related to Young's modulus measured parallel, E_0, and perpendicular, E_{90}, to the draw direction by

$$E_0 = \frac{1}{S_{33}}, \quad E_{90} = \frac{1}{S_{22}}. \quad (7)$$

By writing Equation 6 for $\theta = 45°$ and substituting in Equation 6 we get the simpler form, namely

$$\frac{1}{E_\theta} = \frac{\cos^4\theta}{E_0} + \frac{\sin^4\theta}{E_{90}} + \left(\frac{4}{E_{45}} - \frac{1}{E_0} - \frac{1}{E_{90}}\right)\cos^2\theta\sin^2\theta, \quad (8)$$

which gives the variation of modulus in the plane of the sheets as a function of θ.

3. Experimental

3.1. Preparation and characterization of samples

A low density polyethylene grade "LDPE 1" supplied by the PSCC centre at the Rubber and Plastics Research Association (RAPRA) was used with a melt index of 0.2 g/10 min (BS 2782), a density of 0.920 g cm^{-3}, $M_n = 2.46 \times 10^4$ and $M_w = 2.15 \times 10^5$. Isotropic sheets, approximately 0.25 cm thick, were prepared from granules by compression moulding between aluminium plates at a temperature of 165° C. After complete melting the sheets were allowed to cool slowly for 12 h. Rectangular samples, length 14 cm and width 5 cm, were cut from the pressed sheets and hot-drawn at 85° C at an extension rate of 1 cm min^{-1}. On completion of drawing the sheets were left to cool slowly for 12 h while still at constant extension. A grid of 1 cm squares marked on each sheet prior to drawing was used to determine the draw ratio λ (length between marking after/before drawing) [15]. The method of preparation was intended to produce anisotropic sheets with transverse symmetry about the draw direction. The oriented sheets were stored at room temperature for at least three weeks. Specimens for the relaxation tests, 5.0 cm × 0.5 cm, were cut from the drawn samples with the tensile axis parallel to the drawing direction. Specimens were also cut from

samples having a draw ratio of $\lambda = 2.2$ with their tensile axis at different angles, θ, to the drawing direction.

Isotropic specimens were obtained from a compression-moulded sheet with a thickness of 0.10 cm, annealed at 80° C for 24 h. Some of the hot-drawn sheets were also annealed at 80° C for 12 h at constant extension after completion of the drawing procedure.

Wide angle X-ray photographs were obtained using Ni-filtered CuKα radiation. Transmission diffraction measurements were made using a texture diffractometer scanning the appropriate Debye rings.

3.2. Relaxation measurements

The apparatus used for the relaxation experiments in uniaxial extension has been described elsewhere [14]. The experiments were conducted at constant strain after straining the samples at a strain rate of 1.4×10^{-2} sec^{-1}. The initial strain level was calculated from a knowledge of strain rate and straining time. The initial stress in the stress relaxation experiments was chosen as the stress at zero time, i.e. the stress present at the moment the straining was stopped. The temperature was 24 ± 0.1° C. Most of the experiments were run for approximately 3 h, but in some cases the tests were continued for a longer time.

3.3. Modulus measurements

Tensile modulus values (secant modulus) were obtained from stress–strain diagrams at a constant strain rate of 1.4×10^{-2} sec^{-1}.

4. Results

4.1. WAXS

It has been shown elsewhere that the method of preparation of the anisotropic specimens will result in a material with transverse symmetry [15, 16]. Fig. 1 shows the uncorrected diffractometer traces of the [1 1 0] and [2 0 0] reflections as a function of the rotation angle at various draw ratios. The well-known cone distribution of the [1 1 0] reflections in the cold-drawn materials appears here at low draw ratios. The narrow cone distribution of the *a*-axis as reported elsewhere [5] for the hot-drawn material also appears here at $\lambda = 1.8$ though not well developed.

4.2. Stress–strain curves

In Fig. 2 (left) the stress–strain curves parallel to draw direction for samples with different draw ratios are shown. As can be seen, the modulus increases with increasing draw ratio. The right-hand part of Fig. 2 shows the stress–strain curves at various directions, θ, in relationship to the orientation direction at a draw ratio of $\lambda = 2.2$.

4.3. Variation of modulus with angle

In Fig. 7 the theoretical expression, Equation 8, for the angular dependence of the modulus is compared with experimental results for a specimen with $\lambda = 2.2$. The modulus was obtained from stress–strain diagrams at various angles at strains of 0.3% and 1.5%.

4.4. Stress relaxation in the draw direction

The effect of the draw ratio λ on the overall

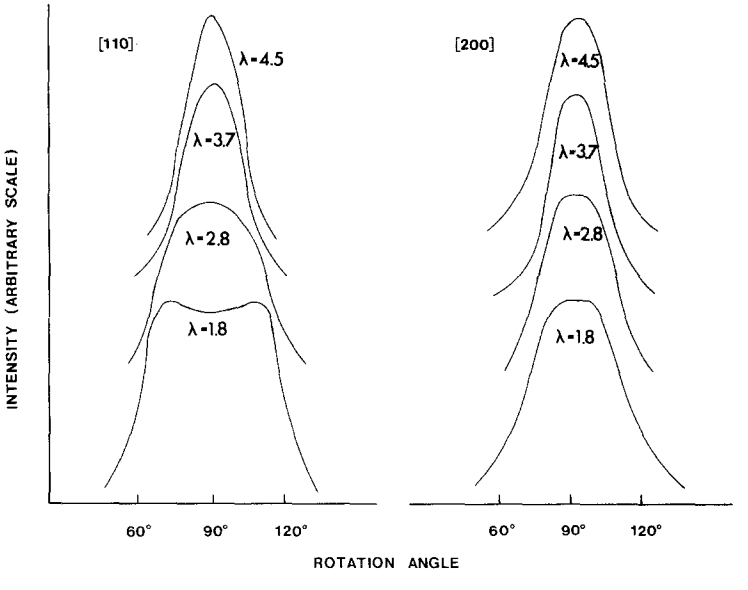

Figure 1 [1 1 0] and [2 0 0] azimuths (uncorrected) for LDPE drawn to indicated draw ratios at 85° C.

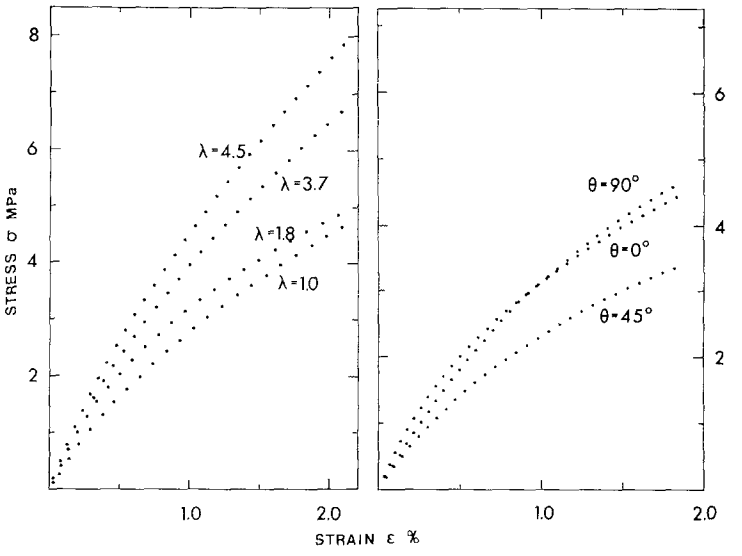

Figure 2 Stress–strain curves parallel to the draw direction for various draw ratios (left) and at different angles to the draw direction, $\lambda = 2.2$ (right). $\dot{\epsilon} = 1.4 \times 10^{-2}$ sec^{-1}.

appearance of stress relaxation curves for LDPE measured in the draw direction is shown in Fig. 3. The experiments were performed after straining the samples to a constant level of approximately 0.2%. The relaxation behaviour of the isotropic material is also included. A comparison of the behaviour of the oriented and the isotropic samples shows that the relaxation curves for the oriented material are all shifted to the left compared to the behaviour of the isotropic material. Furthermore, the internal stress is lowered as a result of the drawing.* This does not occur, however, at the highest draw ratio used ($\lambda = 4.5$).

What has been said about the positions of the curves on the log t axis is also shown in Table I, which gives the elapsed time for reaching a relaxation stress equal to half the initial stress at the beginning of the relaxation process (measurements in the draw direction).

4.5. Angular dependence of stress relaxation ($\lambda = 2.2$)

Typical stress relaxation curves obtained with samples with $\lambda = 2.2$ cut at different angles to the draw direction, θ, are reproduced in Fig. 4. The relaxation curves for the oriented material

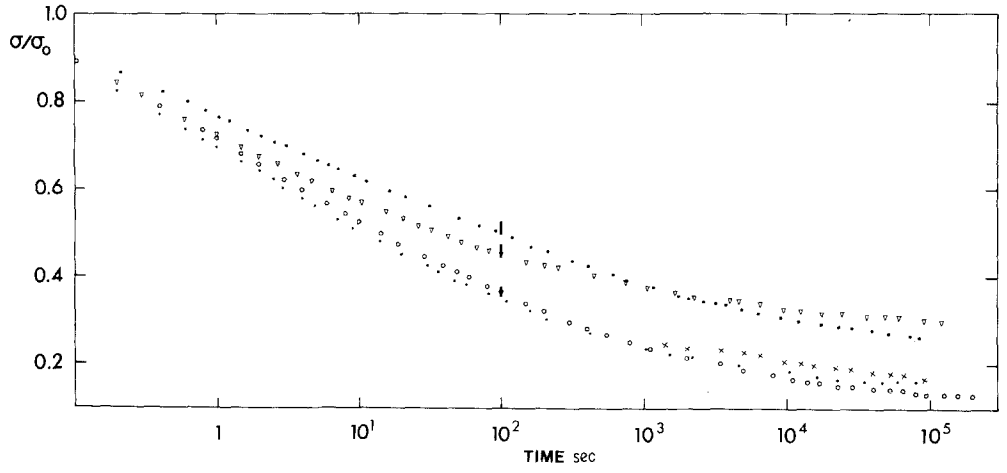

Figure 3 Stress relaxation curves for various draw ratios parallel to the orientation direction. Initial stresses and strains: $\lambda = 1.0$, $\sigma_0 = 0.82$ MPa; $\epsilon_0 = 0.22\%$ (•); $\lambda = 1.8$, $\sigma_0 = 1.02$ MPa, 0.21%(○); $\lambda = 2.4$, $\sigma_0 = 0.79$ MPa, 0.19%(·); $\lambda = 2.8$, $\sigma_0 = 0.88$ MPa, 0.17%(×); $\lambda = 4.5$, $\sigma_0 = 1.22$ MPa, 0.20%(▽). The curve for $\lambda = 2.8$ coincides at $t < 10^3$ sec with the curve for $\lambda = 2.4$. The scatter between 3 and 5 individual measurements is shown as vertical bars.

*The same behaviour was also recorded for oriented samples which had been annealed at 80° C for 12 h at constant extension after completion of the drawing procedure.

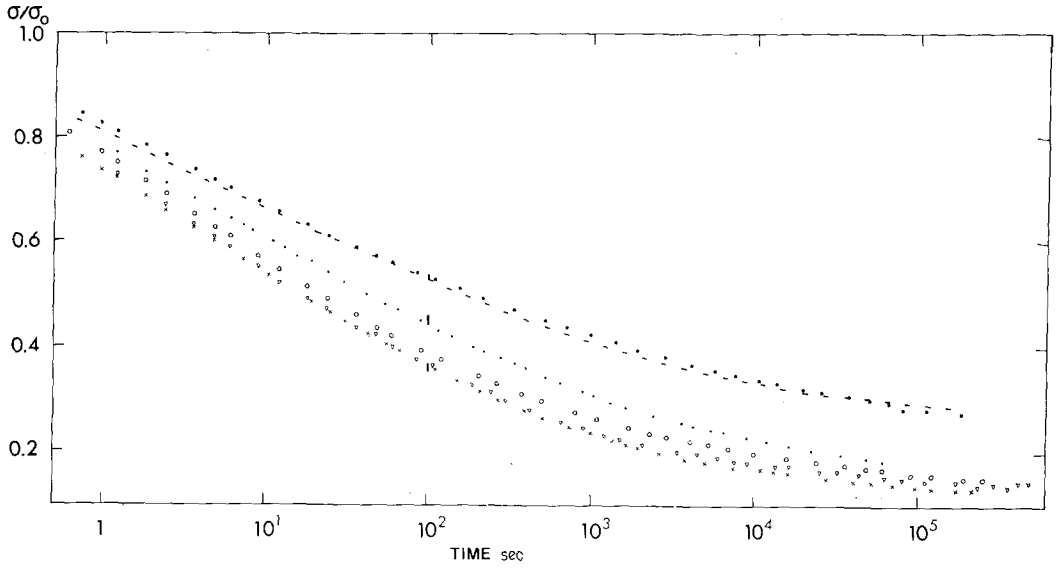

Figure 4 Stress relaxation at various angles, θ, to the orientation direction in the plane of the sheet ($\lambda = 2.2$). Initial stresses and strains: $\theta = 0°$, $\sigma_0 = 2.25$ MPa, $\epsilon_0 = 0.60\%$(○); 20°, $\sigma_0 = 1.34$ MPa, 0.37%(▽); 45° $\sigma_0 = 1.42$ MPa, 0.50% (×); 70°, $\sigma_0 = 1.78$ MPa, 0.58%(·); 90°, $\sigma_0 = 1.72$ MPa, 0.47%(●), and at $\lambda = 1.0$, $\sigma_0 = 1.75$ MPa, 0.54%(—). The scatter between 3 and 5 individual measurements is shown as vertical bars.

TABLE I The time taken for the stress $\sigma(t)$ to drop to half its initial value σ_0 (measurements in the draw direction)

Draw ratio (λ)	Time (sec)
1.0	100–180
1.8	10–20
2.8	10–20
3.7	20–70
4.5	40–100

The longer times refer to higher initial strains, i.e. an increase in strain produces a shift of the σ/σ_0–log t curves to the right on the log t axis.

are shifted to the left compared to the behaviour of the isotropic material. Furthermore, the internal stress is lower in the oriented samples. These effects are similar to that found parallel to the draw direction with samples having different λ values, cf. Fig. 3. However, the 90° sample represents an exception, in that its relaxation behaviour is similar to that found for the isotropic material, both with regard to the position on the log time axis and to the level of internal stress.

Figs. 3 and 4 also show the maximum scatter (vertical bars) between individual curves for some draw ratios and also, at constant λ, for different θ. An effort was made to keep the initial strain constant, the scatter referring to between 3 and 5 individual curves.

4.6. Internal stresses

As it is assumed that the rate of flow in solids depends on the value of the effective stress σ^*, i.e. the difference between the applied and the internal stress ($\sigma^* = \sigma - \sigma_i$), it is natural to include the determination of the internal stress level in the analysis of the relaxation kinetics.

It has earlier been shown that two types of internal stresses affect the relaxation behaviour of polymeric materials [1–3]; permanent stresses originating from moulding conditions, mechanical treatment etc., and stresses induced during the initial deformation of the sample preceding the relaxation experiment. The former type of stress can be determined as follows: The maximum slope F of the σ–ln t curves is plotted versus the initial stress σ_0. The intercept of the resulting straight line with the σ_0 axis gives the value of the permanent internal stress. Fig. 5 shows examples of this procedure applied to samples with varying λ values parallel to the orientation direction. As all the F–σ_0 lines pass through the origin, the samples used can be considered as free from permanent internal stresses. The same is true for the F–σ_0 lines obtained at different angles to the draw direction.

The second component of the internal stress can be determined by a method proposed by Li [1, 2, 17]. The method starts with determining

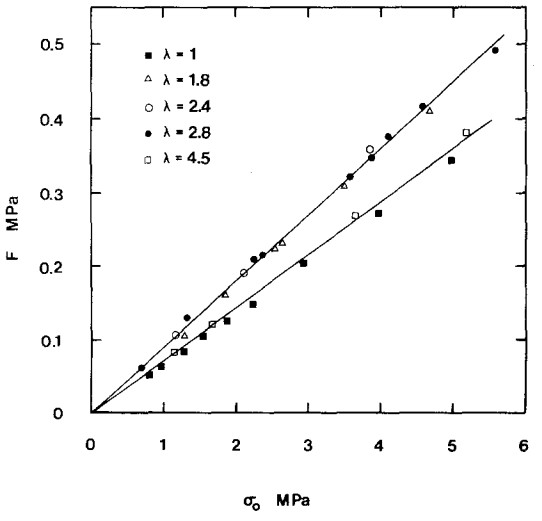

Figure 5 The maximum slope, F, of the σ–ln t curves versus initial stress, σ_0, for draw ratios indicated.

the slope of the σ–ln t curves at different stress levels, whereafter the slope is plotted versus the stress. The intercept of the resulting line with the stress axis is a measure of the internal stress component σ_i. The value of internal stress determined in this way is identified with the stress level that is reached at infinite time (equilibrium stress) [1, 4]. The magnitude of σ_i has been shown to increase with the deformation (stress) applied to the sample [1, 2].

Fig. 6 shows the variation of the strain induced component, σ_i, with the initial stress for various draw ratios (measurements in the draw directions). For a given initial stress, it can be seen that a lower value of the internal stress is obtained in the oriented material (at low draw ratios) compared to the result for the isotropic material. This effect is, however, not observed at the highest draw ratio used ($\lambda = 4.5$).

The internal stress σ_i has also been evaluated for directions differing from the drawing direction for samples with $\lambda = 2.2$. In this case, the initial strain ϵ_0 of the relaxation experiments was kept constant (0.3%). A modulus defined as $E_{i,\theta} = \sigma_i(\theta)/\zeta_0$ was calculated from the σ_i value corresponding to this strain. The angular dependence of this modulus is shown in Fig. 7.

4.7. The activation volume and the exponent n

An important parameter associated with stress relaxation kinetics is the activation volume, v, as it appears in the theory of stress-aided thermal

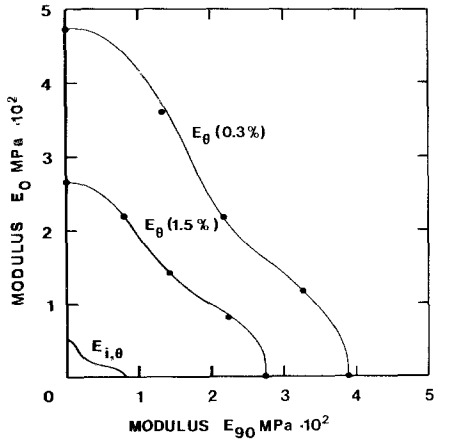

Figure 7 Angular variations of modulus in the plane of the sheet, E_θ, obtained from stress–strain diagrams (·) as a function of θ. Initial strains: 0.3% and 1.5%. The two solid lines are obtained from Equation 8 at $\epsilon_0 = 0.3\%$ and 1.5%. Modulus $E_{i,\theta}$ is defined as $\sigma_i(\theta)/\epsilon_0$ and is shown as a function of $\theta(\epsilon_0 = 0.3\%)$.

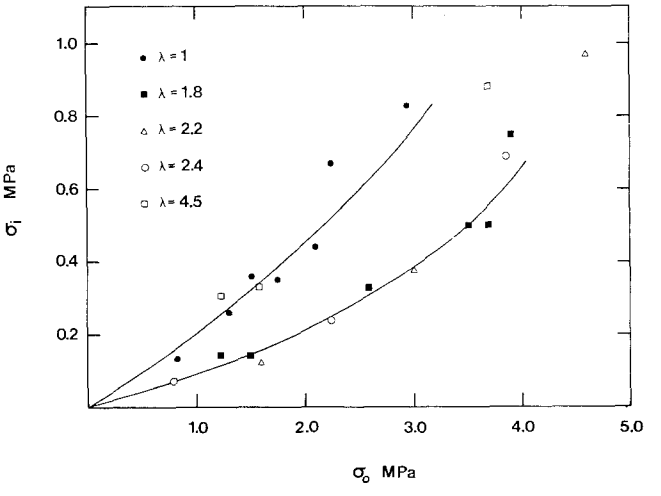

Figure 6 The strain-induced component of the internal stress, σ_i, determined according to Li's method versus initial stress, σ_0, for various draw ratios. The two lines are drawn "by eye" through the experimental points which gives σ_i as a function for σ_0 for $\lambda = 1.0$ and $\lambda = 1.8$ to 2.4.

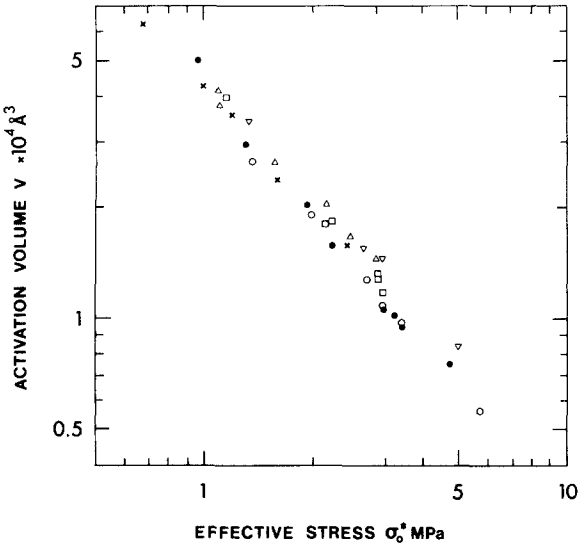

Figure 8 Log–log representation of the dependence of activation volume on the effective initial stress. The activation volume was calculated from the exponential law region. Parallel to the orientation direction: $\lambda = 1.0$ (×); $\lambda = 1.8$ (□); $\lambda = 2.8$ (○); $\lambda = 3.7$ (·); $\lambda = 4.5$ (▽). At different angles to the draw direction; $\lambda = 2.2$, $\theta = 0°, 20°, 45°, 70°, 90°$ (△).

activation. In the present case the value of v was calculated for the curves in Figs. 3 and 4, obtained from samples with different λ values. The calculation, relating to the exponential region of the curves, was based on the usual formula

$$v = kT\left(\frac{\mathrm{d}\ln\dot{\sigma}}{\mathrm{d}\sigma^*}\right)_{T,p} \qquad (9)$$

As evident from Fig. 8, the v value varies inversely with the initial effective stress $\sigma_0^*(\sigma_0^* = \sigma_0 - \sigma_i)$. The constant of proportionality was found to be $\approx 10\,kT$, independent of the draw ratio and in accordance with earlier findings for different solids [1–4].

The stress exponent n of the power law, Equation 2, was evaluated from the slope of the $\mathrm{d}\sigma/\mathrm{d}\ln t$ versus σ plot, which equals $1/(n-1)$. The validity of Equation 2 is shown in Fig. 9. Here $\log(\sigma - \sigma_i)$ is plotted versus $\log t$ for different draw ratios, for sufficiently long times straight lines are obtained. The value of the exponent n, obtained at different draw ratios, is given in Table II.

TABLE II Average value of the exponent "n", determined from the $\mathrm{d}\sigma/\mathrm{d}(\ln t)$ versus σ plot

Draw ratio (λ)	Angle to draw direction θ (degrees)	n
1.0	–	5–6
1.8	0	4–5
2.2	0–70	4–5
	90	5–6
2.4–2.8	0	4–5
3.7	0	5–6
4.5	0	6–7

5. Discussion

The main purpose of this work was to study the influence of orientation on the time dependence of stress relaxation, with special regard to the maximum slope of the σ–$\ln t$ curves and the stress

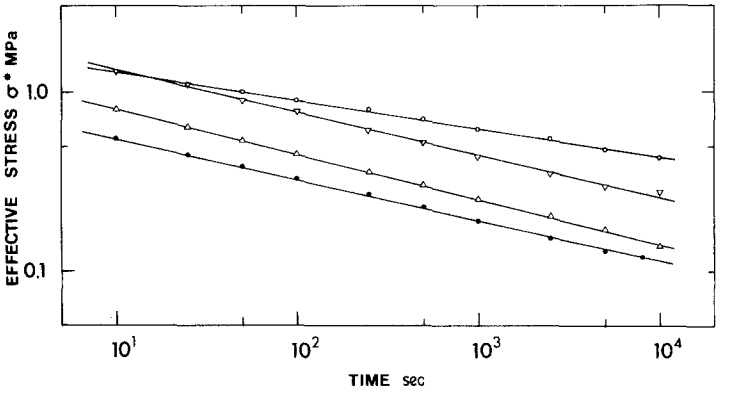

Figure 9 Log–log representation of the dependence of the effective stress on time. The following data are shown: $\lambda = 2.2$, $\sigma_0 = 3.0$ MPa(▽); $\lambda = 2.8$, $\sigma_0 = 2.4$ MPa(△); $\lambda = 3.7$, $\sigma_0 = 1.7$ MPa(·); $\lambda = 4.5$, $\sigma_0 = 4.0$ MPa(○).

level approached after an infinitely long time (the internal stress level). Furthermore, an investigation was made of the position of the relaxation curves along the time axis, as affected by the orientation. It has been shown in Figs. 3 and 4 that a shift of the relaxation curves to shorter times is obtained for the oriented material. Also, as shown in Fig. 6, a lower value of the internal stress (corresponding to a lowering of the equilibrium stress) has been found for the oriented material.

The slope, F, of the linear part of the relaxation curves is found to be related to the initial effective stress as $F \approx 0.1\ \sigma_0^*$, independent of the orientation. This relation has been found valid for a large number of materials with widely differing structures and compositions [1–4]. In this case its validity was confirmed with a material possessing a varying degree of anisotropy. Thus, the main characteristics of the relaxation kinetics are determined by the level of the internal stress, a fact that is clearly demonstrated by the results of this work. This has earlier also been recognized by de Batist and Callens [11] for example, for stress relaxation in metals.

These results can be compared with the reports on creep experiments at room temperature, with oriented LDPE by Darlington and Saunders [5, 18–21].

For the hot-drawn material a higher creep rate was obtained at low draw ratios compared to the isotropic case. Also, it was found that the creep rate was higher in the orientation direction, than perpendicular to this direction. A comparison with the results obtained by Raumann and Saunders [22, 23] for the tensile modulus at room temperature for cold-drawn LDPE, led them to conclude that the type of anisotropy exhibited by the cold-drawn material at the beginning of the creep test, slowly develops in the hot-drawn material during the creep process.

In the present case, the secant modulus obtained from stress–strain diagrams parallel to the draw direction at a constant strain rate $\dot{\epsilon} = 1.4 \times 10^{-2}\ \text{sec}^{-1}$ and $\epsilon_0 = 0.3\%$ was calculated as a function of the degree of orientation, λ. Keeping the strain constant at this value for the samples having different λ values, gives the relaxation modulus $E_r(t) = \sigma(t)/\epsilon_0$ as a function of time and degree of orientation, λ. The results are given in Fig. 10. After relaxation for 100 sec, a minimum in $E(t)$ versus λ is observed. A comparison with Fig. 9 in [5] shows satisfactory agreement. In the present work this behaviour is a combined effect of the shift of the relaxation curves along the time axis to shorter times and the lowering of the internal stress at low draw ratios compared to the isotropic material.

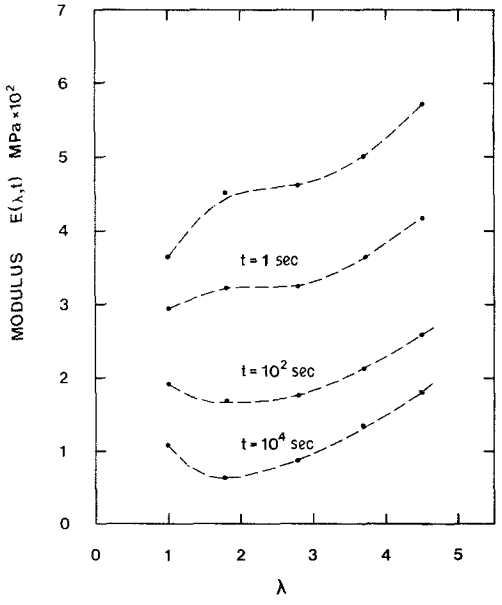

Figure 10 Variation of modulus with draw ratio and relaxation time (initial strain 0.3%). The upper line refers to secant modulus data obtained from stress–strain diagrams at constant strain rate. The lower lines refer to stress relaxation modulus data at constant strain, obtained after relaxation for 1, 100, and 10^4 sec, respectively.

In morphological terms, this finding was explained in [5] by considering the dynamical mechanical properties of oriented LDPE as reported by Ward and Takayanagi [15, 16, 24]. They showed that cold-drawing followed by annealing, which results in a structure of the material similar to that obtained with hot-drawing [5], results in a shift of the viscoelastic transitions, α and β, namely a shift of the α transition (intracrystalline shear process) to higher temperatures and the β transition (interlamellar shear process) to lower temperatures as compared to the cold-drawn case. Thus, the characteristic minimum in the $E(t)$ versus λ relationship for low draw ratios exhibited for cold-drawn material for short time tests and attributed to the intracrystalline shear process [15, 16], will be displayed at longer times (or at higher temperatures) for the hot-drawn material, as is also evident from Fig. 10 in this work.

Finally, some comments on the stress dependence of the activation volume. Using the theory

of stress-aided thermal activation, the stress relaxation properties of LDPE can be analysed with regard to the stress dependence of the activation volume. In this case, the following relation between the activation volume and the initial stress was obtained:

$$v\sigma_0^* = 10kT \qquad (10)$$

The same relation has been shown to apply in stress relaxation for a number of different materials, including polymers and metals [1–4]. The inverse dependence between the activation volume and the initial stress σ_0^* comes from the linearity of the flow rate with respect to initial stress, ($F = 0.1\ \sigma_0^*$, see above), and does not support the idea that the activation volume is determined by structural parameters. Instead there have been attempts to describe the stress relaxation process in terms of co-operative interactions between flow units. The resulting flow equations bear a close similarity to those of stress-aided activation [25–27].

Acknowledgement

The author is indebted to the Swedish Board for Technical Development and to the Swedish Polymer Research Foundation, for financial support. Thanks are also due to Professor J. Kubát for help in preparing the manuscript.

References

1. J. KUBÁT, M. RIGDAHL and R. SELDÉN, *J. Appl. Polymer Sci.* **20** (1976) 2799.
2. J. KUBÁT, R. SELDÉN and M. RIGDAHL, *ibid.* (to be published).
3. J. KUBÁT and M. RIGDAHL, *Phys. Stat. Sol. (a)* **35** (1976) 173.
4. J. KUBÁT, *Nature* **204** (1965) 378.
5. B. H. McCONKEY, M. W. DARLINGTON, D. W. SAUNDERS and C. G. CANNON, *J. Mater. Sci.* **6** (1971) 572, 1474.
6. W. RETTING, 3rd International Conference on Fracture (München F.R.G., 1973).
7. F. JOHANSSON, J. KUBÁT and C. PATTYRANIE, *Ark. Phys.* **28** (1964) 28.
8. H. W. STARKWEATHER, T. F. JORDAN and G. B. DUNNINGTON, *Polymer Eng. Sci.* **14** (1974) 10.
9. D. M. SHINOZAKI, G. W. GROVES and R. G. C. ARRIDGE, *Mater. Sci. Eng.* **28** (1974) 119.
10. R. de BATIST, *Rev. Def. Beh. Mater.* **1** (1975) 2.
11. R. de BATIST and A. CALLENS, *Phys. Stat. Sol. (a)* **21** (1974) 591.
12. A. KAYE and D. W. SAUNDERS, *Brit. J. Appl. Phys.* **15** (1964) 1103.
13. J. F. NYE, "Physical Properties of Crystals" (Clarendon, Oxford, 1957).
14. J. KUBÁT, *Ark. Phys.* **45** (1963) 493.
15. Z. W. STACHURSKI and I. M. WARD, *J. Polymer Sci.* **A-26** (1968) 1083, 1817.
16. *Idem, J. Macromol. Sci. (Phys.)* **B3** (1969) 427, 445.
17. J. C. M. LI, *Can. J. Phys.* **45** (1967) 493.
18. M. W. DARLINGTON and D. W. SAUNDERS, *J. Phys. D. (Appl Phys.)* **3** (1970) 535.
19. D. W. SAUNDERS and M. W. DARLINGTON, *Nature* **218** (1968) 561.
20. M. W. DARLINGTON and D. W. SAUNDERS, *J. Macromol. Sci. (Phys.)* **B5** (1971) 207.
21. *Idem, Polymer Eng. Sci.* **14** (1974) 9.
22. G. RAUMANN and D. W. SAUNDERS, *Proc. Phys. Soc.* **77** (1961) 1028.
23. G. RAUMANN, *ibid.* **79** (1962) 1221.
24. M. TAKAYANAGI, K. IMADA and T. KAJIYAMA, *J. Polymer Sci.* **C15** (1966) 263.
25. Yu. Ya. GOTTLIB, A. V. DOBRODUMOV, A. M. ELYASHEVIC and Yu. E. SVETLOV, *Sov. Phys. Sol. Stat.* **15** (1973) 555.
26. L. BOHLIN and J. KUBÁT, *Sol. Stat. Comm.* **20** (1976) 211.
27. J. KUBÁT and M. RIGDAHL, Proceedings of the British Society of Rheologists, Edinburgh (1977).

Received 13 March and accepted 7 July 1978.